

# Sweeping Preconditioner for the Helmholtz Equation: Moving Perfectly Matched Layers

Björn Engquist and Lexing Ying

Department of Mathematics and ICES, University of Texas, Austin, TX 78712

July 2010

## Abstract

This paper introduces a new sweeping preconditioner for the iterative solution of the variable coefficient Helmholtz equation in two and three dimensions. The algorithms follow the general structure of constructing an approximate  $LDL^t$  factorization by eliminating the unknowns layer by layer starting from an absorbing layer or boundary condition. The central idea of this paper is to approximate the Schur complement matrices of the factorization using moving perfectly matched layers (PMLs) introduced in the interior of the domain. Applying each Schur complement matrix is equivalent to solving a quasi-1D problem with a banded LU factorization in the 2D case and to solving a quasi-2D problem with a multifrontal method in the 3D case. The resulting preconditioner has linear application cost and the preconditioned iterative solver converges in a number of iterations that is essentially indefinite of the number of unknowns or the frequency. Numerical results are presented in both two and three dimensions to demonstrate the efficiency of this new preconditioner.

**Keywords.** Helmholtz equation, perfectly matched layers, high frequency waves, preconditioners,  $LDL^t$  factorization, Green's functions, multifrontal methods, optimal ordering.

**AMS subject classifications.** 65F08, 65N22, 65N80.

## 1 Introduction

This is the second of a series of papers on developing efficient preconditioners for the numerical solutions of the Helmholtz equation in two and three dimensions. To be specific, let the domain of interest be the unit box  $D = (0, 1)^d$  with  $d = 2, 3$ . The time-independent wave field  $u(x)$  for  $x \in D$  satisfies the following Helmholtz equation,

$$\Delta u(x) + \frac{\omega^2}{c^2(x)} u(x) = f(x),$$

where  $\omega$  is the angular frequency,  $c(x)$  is the velocity field and,  $f(x)$  is the external force. Commonly used boundary conditions are the approximations of the Sommerfeld condition which guarantees that the wave field generated by  $f(x)$  propagates out of the domain and other boundary condition for part of the boundary can also be considered. By appropriately rescaling the system, it is convenient to assume that the mean of  $c(x)$  is around 1. Then  $\frac{\omega}{2\pi}$  is the (average) wave number of this problem and  $\lambda = \frac{2\pi}{\omega}$  is the (typical) wavelength.

Equations of the Helmholtz type appear commonly in acoustics, elasticity, electromagnetics, geophysics, and quantum mechanics. Efficient and accurate numerical solution of

the Helmholtz equation is a very important problem in current numerical mathematics. This is, however, a very difficult computational task due to two main reasons. First, in a typical setting, the Helmholtz equation is discretized with at least a constant number of points per wavelength. Therefore, the number of samples  $n$  in each dimension is proportional to  $\omega$ , the total number of samples  $N$  is  $n^d = O(\omega^d)$ , and the approximating discrete system of the Helmholtz equation is an  $O(\omega^d) \times O(\omega^d)$  linear system, which is extremely large in many practical high frequency simulations. Second, since the discrete system is highly indefinite and has a very oscillatory Green's function due to the wave nature of the Helmholtz equation, most direct and iterative solvers developed based on the multiscale paradigm are no longer efficient anymore. For further remarks, see the discussion in [12].

## 1.1 Approach and contribution

In the previous paper [12], we introduced a sweeping preconditioner that constructs an approximate  $LDL^t$  factorization layer by layer starting from an absorbing layer. An important observation regarding the sweeping preconditioner is that the intermediate Schur complement matrices of the  $LDL^t$  factorization corresponds to the restriction of the half-space Green's function of the Helmholtz equation to a single layer. In [12], we represented the intermediate Schur complement matrices of the factorization efficiently in the hierarchical matrix framework [16]. In 2D, the efficiency of this preconditioner is supported by analysis, has linear complexity, and results very small number of iterations when combined with the GMRES solver. In 3D, however, the theoretical justification is lacking and constructing the preconditioner can be more costly.

In this paper, we propose a new sweeping preconditioner that works well in both two and three dimensions. The central idea of this new approach is to represent these Schur complement matrices in terms of *moving perfectly matched layers* introduced in the interior of the domain. Applying these Schur complement matrices then corresponds to inverting a discrete Helmholtz system of a moving PML. Since each moving PML is only of a few grids wide, fast direct algorithms can be leveraged for this task. In 2D, this discrete system of the moving PML layer is a quasi-1D problem and can be solved efficiently using a banded LU factorization in an appropriate ordering. The construction and application costs of the preconditioner are  $O(n^2) = O(N)$  and  $O(n^2) = O(N)$ , respectively. In 3D, the discrete Helmholtz system of the moving PML is a quasi-2D problem and can be solved efficiently using the multifrontal methods. The construction and application costs of the preconditioner are  $O(n^4) = O(N^{4/3})$  and  $O(n^3 \log n) = O(N \log N)$ , respectively. Numerical results show that in both 2D and 3D this new sweeping preconditioner gives rise to iteration numbers that is essentially independent of  $N$  when combined with the GMRES solver. After the construction of the preconditioner, we thus have a linear solution method for the discrete Helmholtz system.

## 1.2 Related work

There has been a vast literature on developing efficient algorithms for the Helmholtz equation. A partial list of significant progresses includes [3, 4, 6, 8, 10, 11, 14, 19, 23, 24]. We refer to the review article [13] and our previous paper [12] for detailed discussion. The brief discussion below is restricted to the ones that are closely related to the approach proposed in this paper.

The most efficient direct methods for solving the discrete Helmholtz systems are the multifrontal methods or their pivoted versions [9, 15, 22]. The multifrontal methods exploit

the locality of the discrete operator and construct an  $LDL^t$  factorization based on a hierarchical partitioning of the domain. The cost of a multifrontal method depends strongly on the number of dimensions. For a 2D problem with  $N = n^2$  unknowns, a multifrontal method takes  $O(N^{3/2})$  flops and  $O(N \log N)$  storage space. The prefactor is usually rather small, making the multifrontal methods effectively the default choice for most 2D Helmholtz problems. However, for a 3D problem with  $N = n^3$  unknowns, a multifrontal method requires  $O(N^2)$  flops and  $O(N^{4/3})$  storage space, which can be very costly for large scale 3D problems.

The approach proposed here essentially reduces the dimensions of the problem by working with  $n$  subproblems with one dimension lower. In the 3D case, for each subproblem, it leverages the effectiveness of the 2D multifrontal methods by solving a quasi-2D problem. The price of this reduction is that we only end up with an approximate inverse. However, this approximate inverse is reasonably accurate and works very well as a preconditioner when combined with standard iterative solvers in all our variable coefficient test cases.

### 1.3 Contents

The rest of this paper is organized as follows. Section 2 presents the new sweeping preconditioner in the 2D case and Section 3 reports the 2D numerical results. We extend this approach to the 3D case in Section 4 and report the 3D numerical results in Section 5. Finally, Section 6 discusses some future directions of this work.

## 2 Preconditioner in 2D

We will first discuss the sweeping factorization in general and then introduce the moving PML.

### 2.1 Discretization and sweeping factorization

Recall that our computational domain in 2D is  $D = (0, 1)^2$ . In order to simplify the discussion, we assume that the Dirichlet zero boundary condition is used on the side  $x_2 = 1$  while approximations to the Sommerfeld boundary condition is enforced on the other three sides. One standard way of incorporating the Sommerfeld boundary condition is to use the perfectly matched layer (PML) [5, 7, 17]. Introduce

$$\sigma_1(t) = \begin{cases} \frac{C}{\eta} \cdot \left(\frac{t-\eta}{\eta}\right)^2 & t \in [0, \eta] \\ 0 & t \in [\eta, 1-\eta] \\ \frac{C}{\eta} \cdot \left(\frac{t-1+\eta}{\eta}\right)^2 & t \in [1-\eta, 1] \end{cases}, \quad \sigma_2(t) = \begin{cases} \frac{C}{\eta} \cdot \left(\frac{t-\eta}{\eta}\right)^2 & t \in [0, \eta] \\ 0 & t \in [\eta, 1] \end{cases}, \quad (1)$$

and

$$s_1(x_1) = \left(1 + i \frac{\sigma_1(x_1)}{\omega}\right)^{-1}, \quad s_2(x_2) = \left(1 + i \frac{\sigma_2(x_2)}{\omega}\right)^{-1}.$$

Here  $\eta$  is typically around one wavelength and  $C$  is an appropriate positive constant independent of  $\omega$ . The PML method replaces  $\partial_1$  with  $s_1(x_1)\partial_1$  and  $\partial_2$  with  $s_2(x_2)\partial_2$ , respectively. This effectively provides a damping layer of width  $\eta$  near the three sides with the

Sommerfeld boundary condition. The resulting equation becomes

$$\begin{aligned} \left( (s_1 \partial_1)(s_1 \partial_1) + (s_2 \partial_2)(s_2 \partial_2) + \frac{\omega^2}{c^2(x)} \right) u &= f & x \in D = (0, 1)^2, \\ u &= 0 & x \in \partial D. \end{aligned}$$

We assume that  $f(x)$  is supported inside  $[\eta, 1 - \eta] \times [\eta, 1]$  (away from the PML). Dividing the above equation by  $s_1(x_1)s_2(x_2)$  results

$$\left( \partial_1 \left( \frac{s_1}{s_2} \partial_1 \right) + \partial_2 \left( \frac{s_2}{s_1} \partial_2 \right) + \frac{\omega^2}{s_1 s_2 c^2(x)} \right) u = f.$$

The main advantage of this equation is its symmetry. We discretize the domain  $[0, 1]^2$  with a Cartesian grid with spacing  $h = 1/(n + 1)$ . The number of points  $n$  in each dimension is proportional to the wave number  $\omega$  since a constant number of points is required for each wavelength. The set of all interior points of this grid is denoted by

$$\mathcal{P} = \{p_{i,j} = (ih, jh) : 1 \leq i, j \leq n\}$$

(see Figure 1 (left)) and the total number of grid points is  $N = n^2$ .

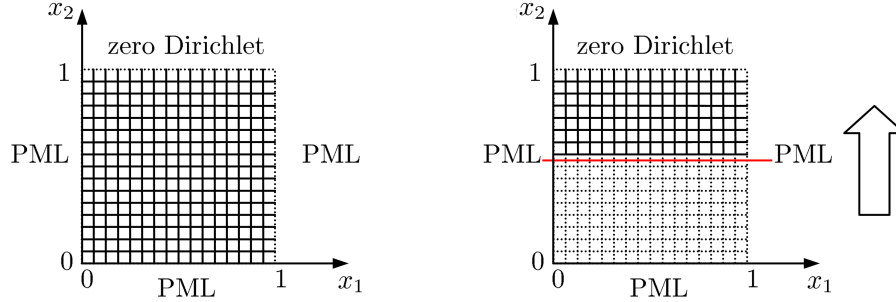


Figure 1: Left: Discretization grid in 2D. Right: Sweeping order in 2D with the moving PML. The dotted grid indicates the part that has already been eliminated.

We denote by  $u_{i,j}$ ,  $f_{i,j}$ , and  $c_{i,j}$  the values of  $u(x)$ ,  $f(x)$ , and  $c(x)$  at point  $p_{i,j} = (ih, jh)$ . The 5-point stencil finite difference method writes down the equation at points in  $\mathcal{P}$  using central difference. The resulting equation at  $x_{i,j} = (ih, jh)$  is

$$\begin{aligned} \frac{1}{h^2} \left( \frac{s_1}{s_2} \right)_{i-\frac{1}{2},j} u_{i-1,j} + \frac{1}{h^2} \left( \frac{s_1}{s_2} \right)_{i+\frac{1}{2},j} u_{i+1,j} + \frac{1}{h^2} \left( \frac{s_2}{s_1} \right)_{i,j-\frac{1}{2}} u_{i,j-1} + \frac{1}{h^2} \left( \frac{s_2}{s_1} \right)_{i,j+\frac{1}{2}} u_{i,j+1} \\ + \left( \frac{\omega^2}{(s_1 s_2)_{i,j} \cdot c_{i,j}^2} - (\dots) \right) u_{i,j} = f_{i,j} \quad (2) \end{aligned}$$

with  $u_{i',j'}$  equal to zero for  $(i', j')$  that violates  $1 \leq i', j' \leq n$ . Here  $(\dots)$  stands for the sum of the four coefficients that appear in the first line. We order both  $u_{i,j}$  and  $f_{i,j}$  row by row starting from the first row  $j = 1$  and define the vectors

$$\begin{aligned} u &= (u_{1,1}, u_{2,1}, \dots, u_{n,1}, \dots, u_{1,n}, u_{2,n}, \dots, u_{n,n})^t, \\ f &= (f_{1,1}, f_{2,1}, \dots, f_{n,1}, \dots, f_{1,n}, f_{2,n}, \dots, f_{n,n})^t. \end{aligned}$$

Denote the discrete system of (2) by  $Au = f$ . We further introduce a block version of it by defining  $\mathcal{P}_m$  to be set of the indices in the  $m$ -th row

$$\mathcal{P}_m = \{p_{1,m}, p_{2,m}, \dots, p_{n,m}\}$$

and introducing

$$u_m = (u_{1,m}, u_{2,m}, \dots, u_{n,m})^t \quad \text{and} \quad f_m = (f_{1,m}, f_{2,m}, \dots, f_{n,m})^t.$$

Then

$$u = (u_1^t, u_2^t, \dots, u_n^t)^t, \quad f = (f_1^t, f_2^t, \dots, f_n^t)^t.$$

Using these notations, the system  $Au = f$  takes the following block tridiagonal form

$$\begin{pmatrix} A_{1,1} & A_{1,2} & & & \\ A_{2,1} & A_{2,2} & \ddots & & \\ & \ddots & \ddots & A_{n-1,n} & \\ & & A_{n,n-1} & A_{n,n} & \end{pmatrix} \begin{pmatrix} u_1 \\ u_2 \\ \vdots \\ u_n \end{pmatrix} = \begin{pmatrix} f_1 \\ f_2 \\ \vdots \\ f_n \end{pmatrix}$$

where  $A_{m,m}$  are tridiagonal and  $A_{m,m-1} = A_{m-1,m}^t$  are diagonal matrices.

The sweeping factorization of the matrix  $A$  is essentially a block  $LDL^t$  factorization that eliminates the unknowns layer by layer, starting from the absorbing layer near  $x_2 = 0$ . The result of this process is a factorization

$$A = L_1 \cdots L_{n-1} \begin{pmatrix} S_1 & & & \\ & S_2 & & \\ & & \ddots & \\ & & & S_n \end{pmatrix} L_{n-1}^t \cdots L_1^t, \quad (3)$$

where  $S_1 = A_{1,1}$ ,  $S_m = A_{m,m} - A_{m,m-1}S_{m-1}^{-1}A_{m-1,m}$  for  $m = 2, \dots, n$ , and  $L_k$  is given by

$$L_k(\mathcal{P}_{k+1}, \mathcal{P}_k) = A_{k+1,k}S_k^{-1}, \quad L_k(\mathcal{P}_i, \mathcal{P}_i) = I \quad (1 \leq i \leq n), \quad \text{and zero otherwise.}$$

This process is illustrated graphically in Figure 1 (right). Inverting this factorization for  $A$  gives the following formula for  $u$ :

$$u = (L_1^t)^{-1} \cdots (L_{n-1}^t)^{-1} \begin{pmatrix} S_1^{-1} & & & \\ & S_2^{-1} & & \\ & & \ddots & \\ & & & S_n^{-1} \end{pmatrix} L_{n-1}^{-1} \cdots L_1^{-1} f.$$

Algorithmically, the construction of the sweeping factorization of  $A$  can be summarized as follows by introducing  $T_m = S_m^{-1}$ .

**Algorithm 2.1.** *Construction of the sweeping factorization of  $A$ .*

- 1:  $S_1 = A_{1,1}$  and  $T_1 = S_1^{-1}$ .
- 2: **for**  $m = 2, \dots, n$  **do**
- 3:    $S_m = A_{m,m} - A_{m,m-1}T_{m-1}A_{m-1,m}$  and  $T_m = S_m^{-1}$ .
- 4: **end for**

Since  $S_m$  and  $T_m$  are in general dense matrices of size  $n \times n$ , the cost of the construction algorithm is of order  $O(n^4) = O(N^2)$ . The computation of  $u = A^{-1}f$  is carried out in the following algorithm once the factorization is ready.

**Algorithm 2.2.** *Computation of  $u = A^{-1}f$  using the sweeping factorization of  $A$ .*

```

1: for  $m = 1, \dots, n$  do
2:    $u_m = f_m$ 
3: end for
4: for  $m = 1, \dots, n - 1$  do
5:    $u_{m+1} = u_{m+1} - A_{m+1,m}(T_m u_m)$ 
6: end for
7: for  $m = 1, \dots, n$  do
8:    $u_m = T_m u_m$ 
9: end for
10: for  $m = n - 1, \dots, 1$  do
11:    $u_m = u_m - T_m(A_{m,m+1}u_{m+1})$ 
12: end for

```

Obviously the computations of  $T_m u_m$  in the second and the third loops only needs to be carried out once for each  $m$ . We prefer to write the algorithm this way for the simplicity of presentation. The cost of computing  $u$  with Algorithm 2.2 is of order  $O(n^3) = O(N^{3/2})$ , which is about  $O(N^{1/2})$  times more expensive compared to the multifrontal method. Therefore, these two algorithms themselves are not very useful.

## 2.2 Moving PML

In Algorithms 2.1 and 2.2, the dominant cost is the construction and the application of the matrices  $T_m$ . In [12], we emphasized the physical meaning of the Schur complement matrices  $T_m$  of the sweeping factorization. Consider only the top-left  $m \times m$  block of the above factorization.

$$\begin{pmatrix} A_{1,1} & A_{1,2} & & \\ A_{2,1} & A_{2,2} & \ddots & \\ & \ddots & \ddots & A_{m-1,m} \\ & & A_{m,m-1} & A_{m,m} \end{pmatrix} = L_1 \cdots L_{m-1} \begin{pmatrix} S_1 & & & \\ & S_2 & & \\ & & \ddots & \\ & & & S_m \end{pmatrix} L_{m-1}^t \cdots L_1^t, \quad (4)$$

where the  $L_k$  matrices are redefined to their restriction to the top-left  $m \times m$  blocks. The matrix on the left is in fact the discrete Helmholtz equation restricted to the half space below  $x_2 = (m+1)h$  and with zero boundary condition on this line. Inverting the factorization (4) gives

$$\begin{pmatrix} A_{1,1} & A_{1,2} & & \\ A_{2,1} & A_{2,2} & \ddots & \\ & \ddots & \ddots & A_{m-1,m} \\ & & A_{m,m-1} & A_{m,m} \end{pmatrix}^{-1} = (L_1^t)^{-1} \cdots (L_{m-1}^t)^{-1} \begin{pmatrix} S_1^{-1} & & & \\ & S_2^{-1} & & \\ & & \ddots & \\ & & & S_m^{-1} \end{pmatrix} L_{m-1}^{-1} \cdots L_1^{-1}.$$

The matrix on the left side is an approximation of the discrete half-space Green's function of the Helmholtz operator with zero boundary condition. On the right side, due to the definition of the matrices  $L_1, \dots, L_{m-1}$ , the  $(m, m)$ -th block of the product is exactly equal to  $S_m^{-1}$ . Therefore,

$T_m = S_m^{-1}$  approximates the discrete half-space Green function of the Helmholtz operator with zero boundary at  $x_2 = (m+1)h$ , restricted to the points on  $x_2 = mh$ .

In the previous paper [12],  $T_m$  is approximated using the hierarchical matrix framework. Due to the fact that the 3D Green's function, restricted to a plane, propagates oscillations in all directions, the theoretical justification of that method is lacking in 3D. Here, we try to approximate the matrix  $T_m$  in a different way.

As an operator,  $T_m : g_m \rightarrow v_m$  maps an external force  $g_m$  loaded only on the  $m$ -th layer to the solution  $v_m$  restricted to the same layer. Though it is a map between quantities only defined on the  $m$ -th layer, the computation domain includes all first  $m$  layers with the PML padded near  $x_2 = 0$ . However, since the force  $g_m$  is only loaded on the  $m$ -th layer, there is no reason to keep the PML layer near  $x_2 = 0$  if one can be satisfied with an approximation.

The central idea is to push the PML from  $x_2 = 0$  right next to  $x_2 = mh$ .

To make this precise, let us assume that the width  $\eta$  of the PML is an integer multiple of  $h$  and let  $b = \eta/h$  be the number of grid points in PML layer in the transversal direction. Define

$$s_2^m(x_2) = \left(1 + i \frac{\sigma_2(x_2 - (m-b)h)}{\omega}\right)^{-1}$$

and introduce an auxiliary problem on the domain  $D_m = [0, 1] \times [(m-b)h, (m+1)h]$ :

$$\begin{aligned} \left( (s_1 \partial_1)(s_1 \partial_1) + (s_2^m \partial_2)(s_2^m \partial_2) + \frac{\omega^2}{c^2(x)} \right) u &= f & x \in D_m, \\ u &= 0 & x \in \partial D_m. \end{aligned} \quad (5)$$

This equation is discretized with the subgrid

$$\mathcal{G}_m = \{p_{i,j}, 1 \leq i \leq n, m-b+1 \leq j \leq m\}$$

of the original grid  $\mathcal{P}$  and the resulting  $bn \times bn$  discrete Helmholtz operator is denoted by  $H_m$ . Following the main idea mentioned above, the operator  $\tilde{T}_m : g_m \rightarrow v_m$  defined through  $H_m$  by

$$\begin{pmatrix} * \\ \vdots \\ * \\ v_m \end{pmatrix} \approx H_m^{-1} \begin{pmatrix} 0 \\ \vdots \\ 0 \\ g_m \end{pmatrix}$$

is an approximation to the matrix  $T_m$ . Notice that applying  $\tilde{T}_m$  to an arbitrary vector  $g_m$  involves solving a linear system of matrix  $H_m$ , which comes from the *local* 5-point stencil on the narrow grid  $\mathcal{G}_m$  that contains only  $b$  layers. Let us introduce a new ordering for  $\mathcal{G}_m$

$$p_{1,m-b+1}, p_{1,m-b+2}, \dots, p_{1,m} \dots p_{n,m-b+1}, p_{n,m-b+2}, \dots, p_{n,m}$$

that iterates through the  $x_2$  direction and denote the permutation matrix induced from this new ordering by  $P_m$ . Now the matrix  $P_m H_m P_m^t$  is a banded matrix with only  $b-1$  lower diagonals and  $b-1$  upper diagonals. It is well known that the LU factorization  $L_m U_m = P_m H_m P_m^t$  can be constructed efficiently. As a result, the application of  $\tilde{T}_m$  can be carried out rapidly.

We call this approach the *moving PML* method, since these new PMLs do not exist in the original problem as they are only introduced in order to approximate  $T_m$  efficiently.

In the above discussion, the moving PML is pushed right next to  $x_2 = mh$ . However, in general we can place the moving PML at a location that is a few layers away from  $x_2 = mh$ . The potential advantage of keeping a few extra layers as a buffer is that the resulting approximation  $\tilde{T}_m$  is more accurate. On the other hand, since there are more layers in the subgrid  $\mathcal{G}_m$  for each  $m$ , the computational cost grows accordingly. In our numerical tests, we observe that extra buffer layers provide little improvement on the approximation accuracy and hence the moving PML is indeed pushed right next to  $x_2 = mh$ .

The application of a PML right next to the layer to be eliminated corresponds to a PML or absorbing boundary condition next to a Dirichlet boundary condition. This has been used as an asymptotic technique for high frequency scattering under the name of on-surface radiation boundary condition (OSRBC) [2, 18]. The OSRBC is an approximation that is more accurate than physical optics but, of course, not as accurate as a full boundary integral formulation.

### 2.3 Approximate inversion and preconditioner

Let us incorporate the moving PML technique into Algorithms 2.1 and 2.2. The computation at the first  $(b+1)$  layers needs to be handled differently, since it does not make sense to introduce moving PML for these initial layers. Let us call the first  $b$  layers the *front* part and define

$$u_F = (u_1^t, \dots, u_b^t)^t \quad \text{and} \quad f_F = (f_1^t, \dots, f_b^t)^t.$$

Then we can rewrite  $Au = f$  as

$$\begin{pmatrix} A_{F,F} & A_{F,b+1} & & & \\ A_{b+1,F} & A_{b+1,b+1} & \ddots & & \\ & \ddots & \ddots & A_{n-1,n} & \\ & & A_{n,n-1} & A_{n,n} & \end{pmatrix} \begin{pmatrix} u_F \\ u_{b+1} \\ \vdots \\ u_n \end{pmatrix} = \begin{pmatrix} f_F \\ f_{b+1} \\ \vdots \\ f_n \end{pmatrix}.$$

The construction of the approximate sweeping factorization of  $A$  takes the following steps. Notice that since  $T_m$  are approximated directly there is no need to compute  $S_m$  anymore.

**Algorithm 2.3.** *Construction of the approximate sweeping factorization of  $A$  with moving PML.*

- 1: Let  $\mathcal{G}_F$  be the subgrid of the first  $b$  layers,  $H_F = A_{F,F}$ , and  $P_F$  be the permutation induce by the new ordering ( $x_2$  first) of  $\mathcal{G}_F$ . Construct the LU factorization  $L_F U_F = P_F H_F P_F^t$ . This factorization implicitly defines  $\tilde{T}_F : \mathbb{C}^{bn} \rightarrow \mathbb{C}^{bn}$ .
- 2: **for**  $m = b+1, \dots, n$  **do**
- 3:   Let  $\mathcal{G}_m = \{p_{i,j}, 1 \leq i \leq n, m-b+1 \leq j \leq m\}$ ,  $H_m$  be the discrete system of (5) on  $\mathcal{G}_m$ , and  $P_m$  be the permutation induced by the new ordering of  $\mathcal{G}_m$ . Construct the LU factorization  $L_m U_m = P_m H_m P_m^t$ . This factorization implicitly defines  $\tilde{T}_m : \mathbb{C}^n \rightarrow \mathbb{C}^n$ .
- 4: **end for**

The cost of Algorithm 2.3 is  $O(b^3 n^2) = O(b^3 N)$ . The computation of  $u \approx A^{-1}f$  using the constructed sweeping factorization is summarized in the following algorithm

**Algorithm 2.4.** *Computation of  $u \approx A^{-1}f$  using the sweeping factorization of  $A$  with moving PML.*

- 1:  $u_F = f_F$  and  $u_m = f_m$  for  $m = b+1, \dots, n$ .



2:  $u_{b+1} = u_{b+1} - A_{b+1,F}(\tilde{T}_F u_F)$ .  $\tilde{T}_F u_F$  is computed as  $P_F^t U_F^{-1} L_F^{-1} P_F u_F$ .  
 3: **for**  $m = b+1, \dots, n-1$  **do**  
 4:    $u_{m+1} = u_{m+1} - A_{m+1,m}(\tilde{T}_m u_m)$ . The application of  $\tilde{T}_m u_m$  is done by forming the vector  $(0, \dots, 0, u_m^t)^t$ , applying  $P_m^t U_m^{-1} L_m^{-1} P_m$  to it, and extracting the value on the last layer.  
 5: **end for**  
 6:  $u_F = \tilde{T}_F u_F$ . See the previous steps for the application of  $\tilde{T}_F$ .  
 7: **for**  $m = b+1, \dots, n$  **do**  
 8:    $u_m = \tilde{T}_m u_m$ . See the previous steps for the application of  $\tilde{T}_m$ .  
 9: **end for**  
 10: **for**  $m = n-1, \dots, b+1$  **do**  
 11:    $u_m = u_m - \tilde{T}_m(A_{m,m+1} u_{m+1})$ . See the previous steps for the application of  $\tilde{T}_m$ .  
 12: **end for**  
 13:  $u_F = u_F - \tilde{T}_F(A_{F,b+1} u_{b+1})$ . See the previous steps for the application of  $\tilde{T}_F$ .  
 The cost of Algorithm 2.4 is  $O(b^2 n^2) = O(b^2 N)$ . Since  $b$  is a fixed constant, the cost is essentially linear. Algorithm 2.4 defines an operator

$$M : f = (f_F^t, f_{b+1}^t, \dots, f_n^t)^t \rightarrow u = (u_F^t, u_{b+1}^t, \dots, u_n^t)^t,$$

which is an approximate inverse of the discrete Helmholtz operator  $A$ . Due to the indefiniteness of  $A$ , this approximate inverse might suffer from instability. In practice, instead of generating the sweeping factorization of the original matrix  $A$ , we choose to generate the factorization for the matrix  $A_\alpha$  associated with the modified Helmholtz equation

$$\Delta u(x) + \frac{(\omega + i\alpha)^2}{c^2(x)} u(x) = f(x), \quad (6)$$

where  $\alpha$  is an  $O(1)$  positive constant. We denote by  $M_\alpha : f \rightarrow u$  the operator defined by Algorithm 2.4 with this modified equation. We would like to emphasize that (6) is very different from the equation used in the shifted Laplacian approach (for example [14, 19]): in the shifted Laplacian formulation the imaginary part of the operator is  $O(\omega)$  while here the imaginary part is  $O(1)$ .

Since  $\alpha$  is small,  $A_\alpha$  is close to  $A$ . Therefore, we propose to solve the preconditioner system

$$M_\alpha A u = M_\alpha f$$

using the GMRES solver [25, 26]. As the cost of applying  $M_\alpha$  to any vector is  $O(n^2) = O(N)$ , the total cost of the iterative solver scales like  $O(N_I N)$ , where  $N_I$  is the number of iterations. As the numerical results in Section 3 demonstrate,  $N_I$  depends at most logarithmically on  $N$ , thus resulting a solver with almost linear complexity.

The problem considered so far has zero Dirichlet boundary condition on  $x_2 = 1$ . A common situation is to impose PML at all sides. In this case, the algorithms need a slight modification. Instead of sweeping upward from  $x_2 = 0$ , the algorithm sweeps with two fronts, one from  $x_2 = 0$  upward and the other from  $x_2 = 1$  downward (see Figure 2 (left)). Similar to  $u_F$  and  $f_F$  near  $x_2 = 0$ , we introduce

$$u_E = (u_{n-b+1}^t, \dots, u_n^t)^t \quad \text{and} \quad f_E = (f_{n-b+1}^t, \dots, f_n^t)^t$$

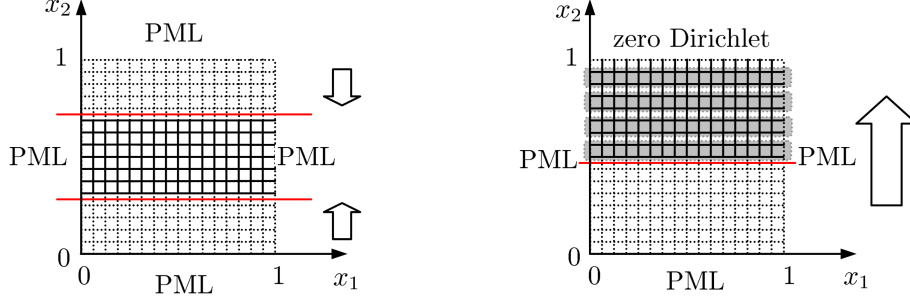


Figure 2: Different sweeping patterns. Left: For problems with PML at both  $x_2 = 0$  and  $x_2 = 1$ , the algorithm sweeps from both ends towards the center. Right: Instead of one layer, multiple layers of unknowns can be eliminated within each iteration of the algorithm.

and write  $Au = f$  in the following block form

$$\begin{pmatrix} A_{F,F} & A_{F,b+1} & & & \\ A_{b+1,F} & A_{b+1,b+1} & \ddots & & \\ & \ddots & \ddots & \ddots & \\ & & \ddots & A_{n-b,n-b} & A_{n-b,E} \\ & & & A_{E,n-b} & A_{E,E} \end{pmatrix} \begin{pmatrix} u_F \\ u_{b+1} \\ \vdots \\ u_{n-b} \\ u_E \end{pmatrix} = \begin{pmatrix} f_F \\ f_{b+1} \\ \vdots \\ f_{n-b} \\ f_E \end{pmatrix}.$$

The upward sweep goes through  $m = F, b+1, \dots, (n-1)/2$ , and the downward sweep visits  $m = E, n-b, \dots, (n+3)/2$ . Finally, the algorithm visits the middle layer  $m = (n+1)/2$  with moving PMLs on both sides.

Algorithm 2.3 eliminates one layer of unknowns within each iteration. We can also instead eliminate several layers of unknowns together within each iteration (see Figure 2 (right)). The resulting algorithm spends more computational time within each elimination step, since the discrete system  $H_m$  contains more layers in the  $x_2$  dimension. On the other hand, the number of elimination steps goes down by a factor equal to the number of layers processed within each elimination step. In practice, the actual number  $d$  of layers processed within each step depends on the width of the moving PML and is chosen to minimize the overall computation time and storage.

### 3 Numerical Results in 2D

In this section, we present several numerical results to illustrate the properties of the sweeping preconditioner described in Section 2. The algorithms are implemented in Matlab and all tests are performed on a computer with a 2.6GHz CPU. We use GMRES as the iterative solver with relative residue tolerance equal to  $10^{-3}$ .

#### 3.1 PML

The examples in this section have the PML boundary condition specified at all sides. We consider three velocity fields in the domain  $D = (0, 1)^2$ :

1. The first velocity field corresponds to a smooth converging lens with a Gaussian profile at the center of the domain (see Figure 3(a)).

2. The second velocity field is a vertical waveguide with Gaussian cross section (see Figure 3(b)).
3. The third velocity field has a random velocity field (see Figure 3(c)).

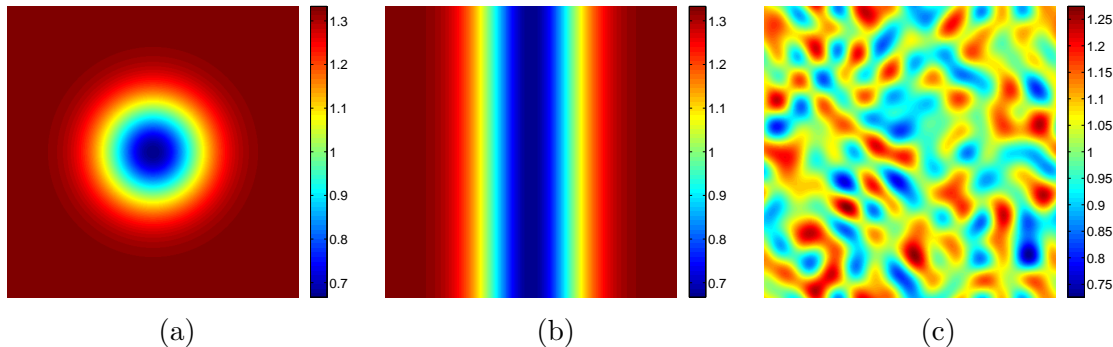


Figure 3: Test velocity fields.

For each velocity field, we test with two external forces  $f(x)$ .

1. The first external force  $f(x)$  is a narrow Gaussian point source located at  $(x_1, x_2) = (0.5, 0.125)$ . The response of this forcing term generates circular waves propagating at all directions. Due to the variations of the velocity field, the circular waves are going to bend, form caustics, and intersect.
2. The second external force  $f(x)$  is a Gaussian wave packet whose wavelength is comparable to the typical wavelength of the domain. This packet centers at  $(x_1, x_2) = (0.125, 0.125)$  and points to the  $(1, 1)$  direction. The response of this forcing term generates a Gaussian beam initially pointing towards the  $(1, 1)$  direction. Due to the variations of the velocity field, this Gaussian beam bends and scatters.

Firstly, we study how the sweeping preconditioner behaves when  $\omega$  varies. For each velocity field, we perform tests for  $\frac{\omega}{2\pi} = 16, 32, \dots, 256$ . In these tests, we discretize each wavelength with  $q = 8$  points and  $n = 127, 255, \dots, 2047$ . The  $\alpha$  value of the modified system is set to be equal to 2. The width of the moving PML is equal to  $12h$  (i.e.  $b = 12$ ) and the number  $d$  of layers processed within each iteration of Algorithms 2.3 and 2.4 is equal to 12. The sweeping pattern indicated in Figure 2 (left) is used in these tests.

The results of the first velocity field are summarized in Table 1.  $T_{\text{setup}}$  denotes the time used to construct the preconditioner in seconds. For each external force,  $N_{\text{iter}}$  is the number of iterations of the preconditioned GMRES iteration and  $T_{\text{solve}}$  is the overall solution time. When  $\omega$  and  $n$  double,  $N$  increases by a factor of 4 and the setup cost in Table 1 increases roughly by a factor of 4 as well, which is consistent with the  $O(N)$  complexity of Algorithm 2.3. At the same time, the number of iterations is essentially independent of  $n$ . As a result, the overall solution time increases by a factor of 4 or 5 when  $N$  quadruples, exhibiting the almost linear complexity of Algorithm 2.4.

The results of the second and third velocity fields are summarized in Tables 2 and 3, respectively. The quantitative behavior of these tests is similar to the one of the first velocity field. In all cases, the GMRES iteration converges in about 20 iterations with the sweeping preconditioner.

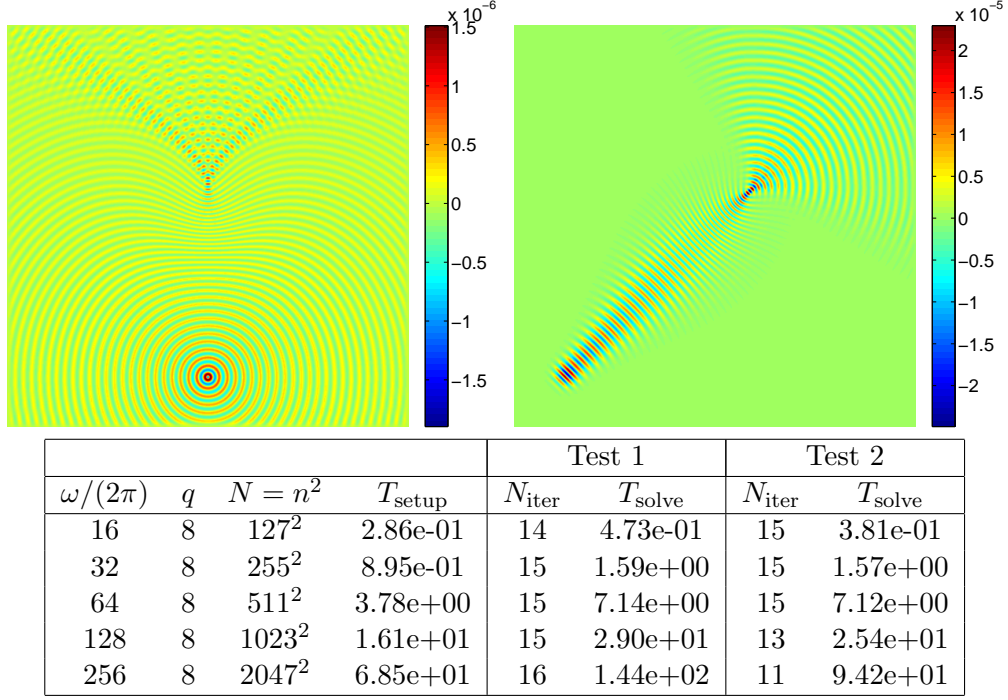


Table 1: Results of velocity field 1 with varying  $\omega$ . Top: Solutions for two external forces with  $\omega/(2\pi) = 64$ . Bottom: Results for different  $\omega$ .

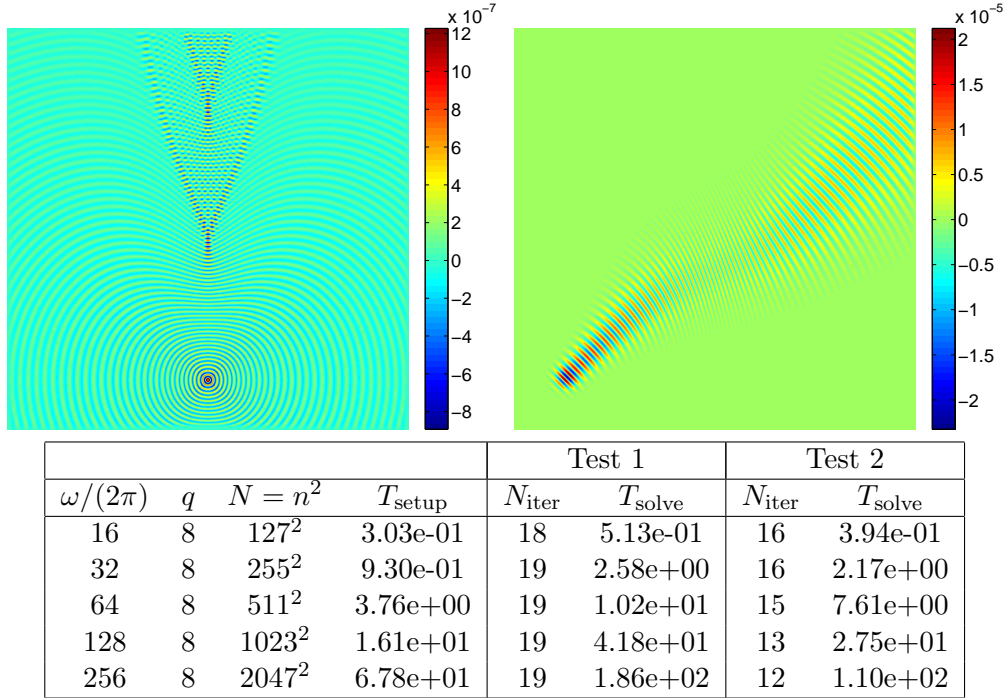
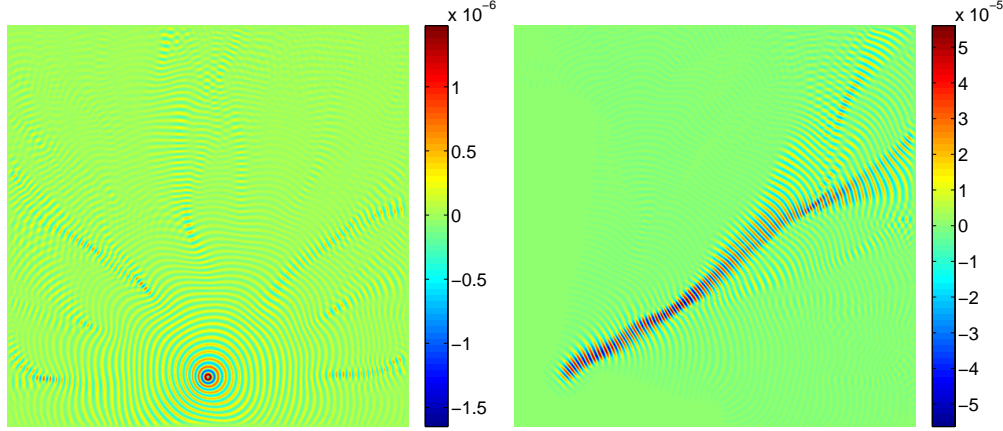


Table 2: Results of velocity field 2 with varying  $\omega$ . Top: Solutions for two external forces with  $\omega/(2\pi) = 64$ . Bottom: Results for different  $\omega$ .



				Test 1		Test 2	
$\omega/(2\pi)$	$q$	$N = n^2$	$T_{\text{setup}}$	$N_{\text{iter}}$	$T_{\text{solve}}$	$N_{\text{iter}}$	$T_{\text{solve}}$
16	8	$127^2$	3.56e-01	18	4.91e-01	19	5.03e-01
32	8	$255^2$	9.31e-01	18	2.42e+00	19	2.61e+00
64	8	$511^2$	3.76e+00	17	8.66e+00	23	1.24e+01
128	8	$1023^2$	1.60e+01	19	3.90e+01	22	4.80e+01
256	8	$2047^2$	6.82e+01	17	1.54e+02	17	1.48e+02

Table 3: Results of velocity field 3 with varying  $\omega$ . Top: Solutions for two external forces with  $\omega/(2\pi) = 64$ . Bottom: Results for different  $\omega$ .

Secondly, we study how the sweeping preconditioner behaves when  $q$  (the number of discretization points per wavelength) varies. We fix  $\frac{\omega}{2\pi}$  to be 32 and let  $q$  be 8, 16, 32, 64. The test results for the three velocity fields are summarized in Tables 4, 5, and 6. These results show that the number of iterations remains to scale at most logarithmically and the running time of the solution algorithm scales roughly linearly with respect to the number of unknowns.

				Test 1		Test 2	
$\omega/(2\pi)$	$q$	$N = n^2$	$T_{\text{setup}}$	$N_{\text{iter}}$	$T_{\text{solve}}$	$N_{\text{iter}}$	$T_{\text{solve}}$
32	8	$255^2$	9.19e-01	15	1.65e+00	15	1.61e+00
32	16	$511^2$	3.91e+00	14	6.94e+00	15	7.22e+00
32	32	$1023^2$	1.59e+01	17	8.87e+01	17	9.39e+01
32	64	$2047^2$	6.68e+01	19	3.74e+02	20	4.15e+02

Table 4: Results of velocity field 1 with varying  $q$ .

Let us compare these numerical results with the ones from the previous paper [12]. The algorithms proposed in this paper are implemented in Matlab, while the ones in [12] are implemented in C++ with compiler optimization. Hence, direct comparison of the running time is clearly in favor of the algorithms in the previous paper. We would expect the running time of the algorithms in this paper to improve by a factor of 2 to 3 when implemented in optimized C++ code. Even with this implementational disadvantage, the setup time  $T_{\text{setup}}$  of the current approach is about twenty times faster. This is mainly due to the fact that the implementation of the LU factorization is much more efficient compared

				Test 1		Test 2	
$\omega/(2\pi)$	$q$	$N = n^2$	$T_{\text{setup}}$	$N_{\text{iter}}$	$T_{\text{solve}}$	$N_{\text{iter}}$	$T_{\text{solve}}$
32	8	$255^2$	9.28e-01	19	2.14e+00	16	1.73e+00
32	16	$511^2$	3.69e+00	17	1.29e+01	15	1.13e+01
32	32	$1023^2$	1.58e+01	24	1.13e+02	15	7.16e+01
32	64	$2047^2$	6.63e+01	26	5.29e+02	17	3.47e+02

Table 5: Results of velocity field 2 with varying  $q$ .

				Test 1		Test 2	
$\omega/(2\pi)$	$q$	$N = n^2$	$T_{\text{setup}}$	$N_{\text{iter}}$	$T_{\text{solve}}$	$N_{\text{iter}}$	$T_{\text{solve}}$
32	8	$255^2$	1.00e+00	16	1.73e+00	16	1.81e+00
32	16	$511^2$	3.66e+00	14	1.34e+01	18	1.87e+01
32	32	$1023^2$	1.52e+01	18	8.16e+01	19	9.22e+01
32	64	$2047^2$	6.57e+01	19	3.99e+02	21	4.62e+02

Table 6: Results of velocity field 3 with varying  $q$ .

to our implementation of the hierarchical matrix algebra in [12]. On the other hand, the number of iterations  $N_{\text{iter}}$  and solution time  $T_{\text{solve}}$  of the current algorithms are higher. This is because in [12]  $T_m$  are represented by numerical low-rank approximations of the full half-space Green's function while in the current approach  $T_m$  are approximated based on a modified Helmholtz equation in a truncated domain.

### 3.2 Scattering problem

The sweeping preconditioner proposed in this paper can also be extended to scattering problems. Let us consider a simple case where the scatterer is a sound soft disk centered at the origin with radius  $r_0$ . In polar coordinates, the scattered field satisfies the following equations

$$\frac{1}{r} (ru_r)_r + \frac{1}{r^2} u_{\theta\theta} + \frac{w^2}{c^2(r, \theta)} u = f$$

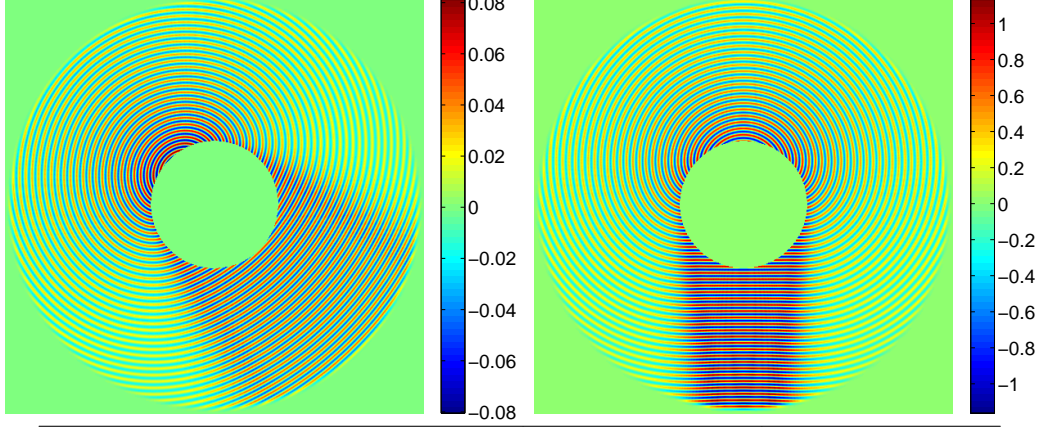
$$u(r_0, \theta) = -u_{\text{inc}}(r_0, \theta),$$

where  $u_{\text{inc}}$  is the incident field and the Sommerfeld boundary condition is specified for  $r$  goes to infinity. One way to solve this scattering problem is to truncate the domain at  $r = r_1$  for some  $r_1 > r_0$  and apply the PML condition at  $r = r_1$ . We can then apply the sweeping preconditioner in the radial direction from  $r = r_1$  to  $r = r_0$ . In the following example,  $c(r, \theta) = 1$ ,  $r_0 = 0.15$  and  $r_1 = 0.5$ . The polar grid is determined so that the each wavelength is discretized with  $q = 8$  points. For each fixed  $\omega$ , two incident fields are used: one is the Green's function centered at  $(-0.2, 0.2)$  and the other is the plane wave  $\exp(-i\omega x_2)$  traveling towards the negative  $x_2$  direction. We perform tests for  $\frac{w}{2\pi} = 16, 32, 64, 128, 256$  and the numerical results are reported in Table 7.

## 4 Preconditioner in 3D

The presentation of the 3D preconditioner follows the layout of the 2D case.





				Incident field 1		Incident field 2	
$\omega/(2\pi)$	$q$	$N$	$T_{\text{setup}}$	$N_{\text{iter}}$	$T_{\text{solve}}$	$N_{\text{iter}}$	$T_{\text{solve}}$
16	8	$45 \times 403$	6.11e-01	7	3.61e-01	7	2.25e-01
32	8	$90 \times 805$	2.61e+00	7	1.11e+00	7	1.11e+00
64	8	$180 \times 1609$	1.17e+01	7	4.92e+00	7	4.90e+00
128	8	$359 \times 3217$	4.95e+01	7	2.10e+01	7	2.06e+01
256	8	$717 \times 6434$	1.99e+02	7	9.01e+01	7	9.00e+01

Table 7: Results of the scattering problem. Top: Scattered fields for two incident waves with  $\omega/(2\pi) = 64$ . Bottom: Results for different  $\omega$ .

#### 4.1 Discretization and sweeping factorization

The computational domain is  $D = (0, 1)^3$ . Similar to the 2D case, assume that the Dirichlet boundary condition is used on the side  $x_3 = 1$  and the Sommerfeld boundary condition is enforced on other sides. Define

$$\sigma_1(t) = \sigma_2(t) = \begin{cases} \frac{C}{\eta} \cdot \left(\frac{t-\eta}{\eta}\right)^2 & t \in [0, \eta] \\ 0 & t \in [\eta, 1-\eta] \\ \frac{C}{\eta} \cdot \left(\frac{t-1+\eta}{\eta}\right)^2 & t \in [1-\eta, 1] \end{cases}, \quad \sigma_3(t) = \begin{cases} \frac{C}{\eta} \cdot \left(\frac{t-\eta}{\eta}\right)^2 & t \in [0, \eta] \\ 0 & t \in [\eta, 1] \end{cases},$$

and

$$s_1(x_1) = \left(1 + i \frac{\sigma(x_1)}{\omega}\right)^{-1}, \quad s_2(x_2) = \left(1 + i \frac{\sigma(x_2)}{\omega}\right)^{-1}, \quad s_3(x_3) = \left(1 + i \frac{\sigma(x_3)}{\omega}\right)^{-1}.$$

The PML approach replaces  $\partial_1$ ,  $\partial_2$ , and  $\partial_3$  with  $s_1(x_1)\partial_1$ ,  $s_2(x_2)\partial_2$ , and  $s_3(x_3)\partial_3$ , respectively. This effectively provides a damping layer of width  $\eta$  near the sides with Sommerfeld condition. The resulting equation takes the form

$$\begin{aligned} \left( (s_1\partial_1)(s_1\partial_1) + (s_2\partial_2)(s_2\partial_2) + (s_3\partial_3)(s_3\partial_3) + \frac{\omega^2}{c^2(x)} \right) u &= f \quad x \in (0, 1)^3, \\ u &= 0 \quad x \in \partial([0, 1]^3). \end{aligned}$$

We assume that  $f(x)$  is supported inside  $[\eta, 1-\eta] \times [\eta, 1-\eta] \times [\eta, 1]$  (away from the PML). Dividing the above equation by  $s_1(x_1)s_2(x_2)s_3(x_3)$  results

$$\left( \partial_1 \left( \frac{s_1}{s_2 s_3} \partial_1 \right) + \partial_2 \left( \frac{s_2}{s_1 s_3} \partial_2 \right) + \partial_3 \left( \frac{s_3}{s_1 s_2} \partial_3 \right) + \frac{\omega^2}{s_1 s_2 s_3 c^2(x)} \right) u = f.$$

The domain  $[0, 1]^3$  is discretized with a Cartesian grid with spacing  $h = 1/(n + 1)$ , where the number of points  $n$  in each dimension is proportional to  $\omega$ . The interior points of this grid are

$$\mathcal{P} = \{p_{i,j,k} = (ih, jh, kh) : 1 \leq i, j, k \leq n\}$$

(see Figure 4 (left)) and the total number of grid points is  $N = n^3$ .

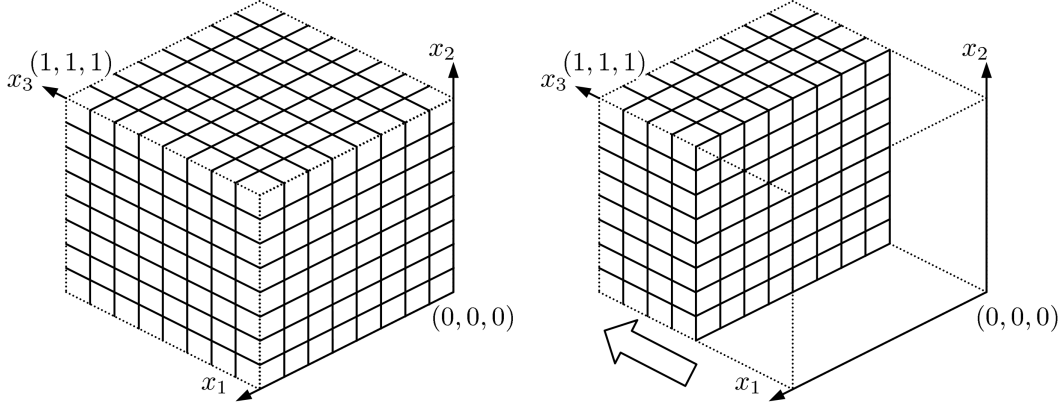


Figure 4: Left: Discretization grid in 3D. Right: Sweeping order in 3D. The remaining grid shows the unknowns yet to be processed.

We denote by  $u_{i,j,k}$ ,  $f_{i,j,k}$ , and  $c_{i,j,k}$  the values of  $u(x)$ ,  $f(x)$ , and  $c(x)$  at point  $x_{i,j,k} = (ih, jh, kh)$ . The standard 7-point stencil finite difference method writes down the equation at points in  $\mathcal{P}$  using central difference. The resulting equation at  $(ih, jh, kh)$  is

$$\begin{aligned} & \frac{1}{h^2} \left( \frac{s_1}{s_2 s_3} \right)_{i-\frac{1}{2},j,k} u_{i-1,j,k} + \frac{1}{h^2} \left( \frac{s_1}{s_2 s_3} \right)_{i+\frac{1}{2},j,k} u_{i+1,j,k} + \frac{1}{h^2} \left( \frac{s_2}{s_1 s_3} \right)_{i,j-\frac{1}{2},k} u_{i,j-1,k} \\ & + \frac{1}{h^2} \left( \frac{s_2}{s_1 s_3} \right)_{i,j+\frac{1}{2},k} u_{i,j+1,k} + \frac{1}{h^2} \left( \frac{s_3}{s_1 s_2} \right)_{i,j,k-\frac{1}{2}} u_{i,j,k-1} + \frac{1}{h^2} \left( \frac{s_3}{s_1 s_2} \right)_{i,j,j+\frac{1}{2}} u_{i,j,k+1} \\ & + \left( \frac{\omega^2}{(s_1 s_2 s_3)_{i,j,k} \cdot c_{i,j,k}^2} - (\dots) \right) u_{i,j,k} = f_{i,j,k} \quad (7) \end{aligned}$$

with  $u_{i',j',k'}$  equal to zero for  $(i', j', k')$  that violates  $1 \leq i', j', k' \leq n$ . Here  $(\dots)$  stands for the sum of the six coefficients appeared in the first two lines. We order  $u_{i,j,k}$  and  $f_{i,j,k}$  by going through the three dimensions in order and denote the vectors containing by

$$\begin{aligned} u &= (u_{1,1,1}, u_{2,1,1}, \dots, u_{n,1,1}, \dots, u_{1,n,n}, u_{2,n,n}, \dots, u_{n,n,n})^t \\ f &= (f_{1,1,1}, f_{2,1,1}, \dots, f_{n,1,1}, \dots, f_{1,n,n}, f_{2,n,n}, \dots, f_{n,n,n})^t \end{aligned}$$

The discrete system of (7) takes the form  $Au = f$ . We further introduce a block version. Define  $\mathcal{P}_m$  to be the indices in the  $m$ -th row

$$\mathcal{P}_m = \{p_{1,1,m}, p_{2,1,m}, \dots, p_{n,n,m}\}$$

and introduce

$$u_m = (u_{1,1,m}, u_{2,1,m}, \dots, u_{n,n,m})^t \quad \text{and} \quad f_m = (f_{1,1,m}, f_{2,1,m}, \dots, f_{n,n,m})^t.$$



Then

$$u = (u_1^t, u_2^t, \dots, u_n^t)^t, \quad f = (f_1^t, f_2^t, \dots, f_n^t)^t.$$

Using these notations, the system  $Au = f$  takes the following block tridiagonal form

$$\begin{pmatrix} A_{1,1} & A_{1,2} & & & \\ A_{2,1} & A_{2,2} & \ddots & & \\ & \ddots & \ddots & A_{n-1,n} & \\ & & A_{n,n-1} & A_{n,n} & \end{pmatrix} \begin{pmatrix} u_1 \\ u_2 \\ \vdots \\ u_n \end{pmatrix} = \begin{pmatrix} f_1 \\ f_2 \\ \vdots \\ f_n \end{pmatrix}$$

where each block is of size  $n^2 \times n^2$  and the off-diagonal blocks are diagonal matrices. The sweeping factorization takes the same form as the 2D one (3). In order to design an efficient preconditioner, the main task is to construct approximations for the Schur complement matrix  $T_m : g_m \rightarrow v_m$ , which maps an external force  $g_m$  loaded only on the  $m$ -th layer to the solution  $v_m$  restricted to the same layer. Following the central idea of pushing the PML right next to  $x_3 = mh$ , we define

$$s_3^m(x_3) = \left( 1 + i \frac{\sigma_3(x_3 - (m-b)h)}{\omega} \right)^{-1}.$$

and introduce an auxiliary problem on the domain  $D_m = [0, 1] \times [0, 1] \times [(m-b)h, (m+1)h]$ :

$$\begin{aligned} \left( (s_1 \partial_1)(s_1 \partial_1) + (s_2 \partial_2)(s_2 \partial_2) + (s_3^m \partial_3)(s_3^m \partial_3) + \frac{\omega^2}{c^2(x)} \right) u &= f & x \in D_m, \\ u &= 0 & x \in \partial D_m. \end{aligned} \quad (8)$$

This equation is then discretized with the subgrid

$$\mathcal{G}_m = \{p_{i,j,k}, 1 \leq i, j \leq n, m-b+1 \leq k \leq m\}$$

of the original grid  $\mathcal{P}$ . The resulting  $bn^2 \times bn^2$  discrete Helmholtz operator is denoted by  $H_m$ . The operator  $\tilde{T}_m : g_m \rightarrow v_m$  defined by

$$\begin{pmatrix} * \\ \vdots \\ * \\ v_m \end{pmatrix} \approx H_m^{-1} \begin{pmatrix} 0 \\ \vdots \\ 0 \\ g_m \end{pmatrix}$$

is an approximation of the Schur complement matrix  $T_m$ . Since  $H_m$  comes from the 7-point stencil with  $b$  layers, this can be viewed as a quasi-2D problem, which can be solved efficiently using a modified version of the multifrontal method [9, 15, 22].

The main idea of the multifrontal method is simple yet elegant. Take a  $n \times n$  2D grid as an example and use  $M$  to denote the discrete operator resulted from a local stencil. The multifrontal method reorders the unknowns hierarchically in order to minimize the fill-ins of the  $LDL^t$  factorization of  $M$ . For the  $n \times n$  Cartesian grid, one possible ordering is given in Figure 5 where the unknowns are clustered into groups and the groups are ordered hierarchically. The construction of the  $LDL^t$  factorization eliminates the unknowns group by group. The dominating cost of the algorithm is spent in inverting the unknowns of the last few groups and the overall cost is  $O(n^3)$ , cubic in terms of the size of the last group. Moreover, the  $L$  matrix is never constructed explicitly in the multifrontal method. Instead

it is stored and applied as a sequence of (block) row operations for the sake of efficiency. Applying  $M^{-1}$  to an arbitrary vector using the result of the multifrontal algorithm takes  $O(n^2 \log n)$  steps. In the current setting, we adopt the same hierarchical partitioning in the  $(x_1, x_2)$  plane, while keeping the unknowns with the same  $x_1$  and  $x_2$  indices in the same group. Since now the size of the last group is of order  $O(bn)$ , the construction phase of the multifrontal method takes  $O(b^3 n^3)$  steps and applying to an arbitrary vector takes  $O(b^2 n^2 \log n)$  steps.

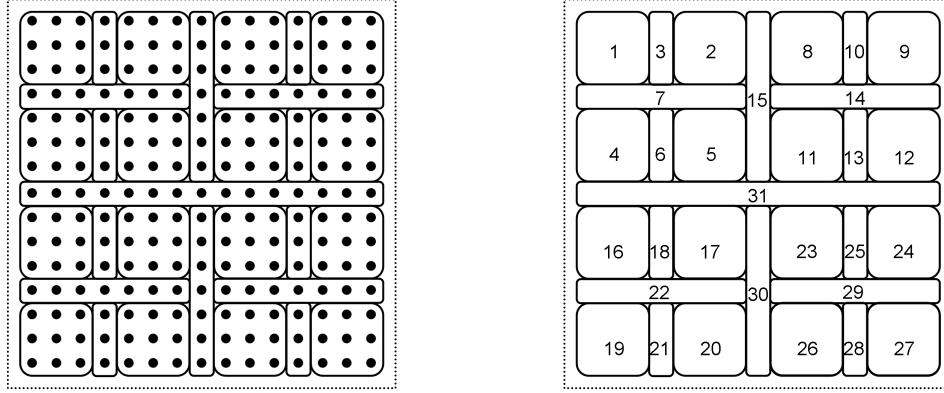


Figure 5: Multifrontal algorithm on a  $15 \times 15$  two dimensional Cartesian grid. Left: The unknowns are clustered into groups hierarchically to minimize the boundary between different groups. Right: Elimination order of different groups. The groups are eliminated in the increasing order of their indices.

## 4.2 Approximate inversion and preconditioner

Let us now combine the multifrontal method into Algorithms 2.1 and 2.2 to build the approximate inverse of  $H$ . Similar to the 2D case, we define

$$u_F = (u_1^t, \dots, u_b^t)^t \quad f_F = (f_1^t, \dots, f_b^t)^t.$$

and write

$$\begin{pmatrix} A_{F,F} & A_{F,b+1} & & & \\ A_{b+1,F} & A_{b+1,b+1} & \ddots & & \\ & \ddots & \ddots & A_{n-1,n} & \\ & & A_{n,n-1} & A_{n,n} & \end{pmatrix} \begin{pmatrix} u_F \\ u_{b+1} \\ \vdots \\ u_n \end{pmatrix} = \begin{pmatrix} f_F \\ f_{b+1} \\ \vdots \\ f_n \end{pmatrix}.$$

The goal of the construction of the approximate sweeping factorization of  $A$  is to compute  $\tilde{T}_m$  and the algorithm consists of the following steps.

**Algorithm 4.1.** *Construction of the approximate sweeping factorization of  $A$  with moving PML.*

- 1: Let  $\mathcal{G}_F$  be the subgrid of the first  $b$  layers and  $H_F = A_{F,F}$ . Construct the multifrontal factorization of  $H_F$  by partitioning  $\mathcal{G}_F$  hierarchically in the  $(x_1, x_2)$  plane.
- 2: **for**  $m = b + 1, \dots, n$  **do**

- 3: Let  $\mathcal{G}_m = \{p_{i,j,k}, 1 \leq i, j \leq n, m-b+1 \leq k \leq m\}$  and  $H_m$  be the system of (8) on  $\mathcal{G}_m$ . Construct the multifrontal factorization of  $H_m$  by partitioning  $\mathcal{G}_m$  hierarchically in the  $(x_1, x_2)$  plane.
- 4: **end for**

The cost of Algorithm 4.1 is  $O(b^3 n^4) = O(b^3 N^{4/3})$ . The computation of  $u$  from this sweeping factorization is summarized in the following algorithm

**Algorithm 4.2.** *Computation of  $u \approx A^{-1}f$  using the sweeping factorization of  $A$  with moving PML.*

- 1:  $u_F = f_F$  and  $u_m = f_m$  for  $m = b+1, \dots, n$ .
- 2:  $u_{b+1} = u_{b+1} - A_{b+1,F}(\tilde{T}_F u_F)$ .  $\tilde{T}_F u_F$  is computed using the multifrontal factorization of  $H_F$ .
- 3: **for**  $m = b+1, \dots, n-1$  **do**
- 4:  $u_{m+1} = u_{m+1} - A_{m+1,m}(\tilde{T}_m u_m)$ . The application of  $\tilde{T}_m u_m$  is done by forming the vector  $(0, \dots, 0, u_m^t)^t$ , applying  $H_m^{-1}$  to it using the multifrontal factorization of  $H_m$ , and extracting the value on the last layer.
- 5: **end for**
- 6:  $u_F = \tilde{T}_F u_F$ . See the previous steps for the application of  $\tilde{T}_F$ .
- 7: **for**  $m = b+1, \dots, n$  **do**
- 8:  $u_m = \tilde{T}_m u_m$ . See the previous steps for the application of  $\tilde{T}_m$ .
- 9: **end for**
- 10: **for**  $m = n-1, \dots, b+1$  **do**
- 11:  $u_m = u_m - \tilde{T}_m(A_{m,m+1} u_{m+1})$ . See the previous steps for the application of  $\tilde{T}_m$ .
- 12: **end for**
- 13:  $u_F = u_F - \tilde{T}_F(A_{F,b+1} u_{b+1})$ . See the previous steps for the application of  $\tilde{T}_F$ .

The cost of Algorithm 4.2 is  $O(b^2 n^3 \log n) = O(b^2 N \log N)$ .

For the stability reason mentioned in Section 2, we apply Algorithms 4.1 and 4.2 to the discrete operator  $A_\alpha$  of the modified system

$$\Delta u(x) + \frac{(\omega + i\alpha)^2}{c^2(x)} u(x) = f(x),$$

where  $\alpha$  is an  $O(1)$  positive constant. We denote by  $M_\alpha : f \rightarrow u$  the operator defined by Algorithm 2.4 for this modified equation. Since  $A_\alpha$  is close to  $A$  when  $\alpha$  is small, we propose to solve the preconditioner system

$$M_\alpha A u = M_\alpha f$$

using the GMRES solver [25, 26]. Because the cost of applying  $M_\alpha$  to any vector is  $O(N \log N)$ , the total cost of the GMRES solver is  $O(N_I N \log N)$ , where  $N_I$  is the number of iterations required. As the numerical results in Section 5 demonstrate,  $N_I$  is essentially independent of the number of unknowns  $N$ , thus resulting an algorithm with almost linear complexity.

## 5 Numerical Results in 3D

In this section, we present several numerical results to illustrate the properties of the algorithm described in Section 4. We use GMRES as the iterative solver with relative residue tolerance equal to  $10^{-3}$ .

The examples in this section have the PML boundary condition specified at all sides. We consider three velocity fields in the domain  $D = (0, 1)^3$ :

1. The first velocity field is a converging lens with a Gaussian profile at the center of the domain (see Figure 6(a)).
2. The second velocity field is a vertical waveguide with Gaussian cross section (see Figure 6(b)).
3. The third velocity field is a random velocity field (see Figure 6(c)).

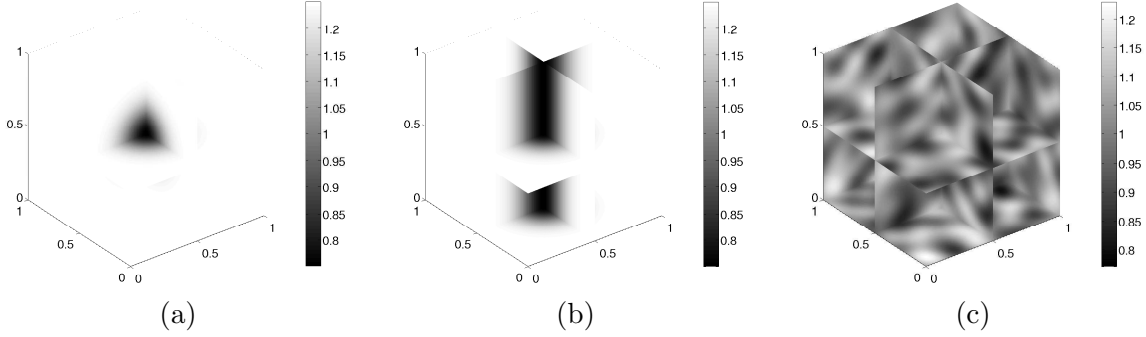


Figure 6: Test velocity fields.

For each problem, we test with two external forces  $f(x)$ .

1. The first external force  $f(x)$  is a Gaussian point source located at  $(x_1, x_2, x_3) = (0.5, 0.5, 0.25)$ . The response of this forcing term generates circular waves propagating at all directions. Due to the variations of the velocity field, the circular waves are going to bend and form caustics.
2. The second external force  $f(x)$  is a Gaussian wave packet whose wavelength is comparable to the typical wavelength of the domain. This packet centers at  $(x_1, x_2, x_3) = (0.5, 0.25, 0.25)$  and points to the  $(0, 1, 1)$  direction. The response of this forcing term generates a Gaussian beam initially pointing towards the  $(0, 1, 1)$  direction.

Firstly, we study how the sweeping preconditioner behaves when  $\omega$  varies. For each velocity field, we perform tests for  $\frac{\omega}{2\pi}$  equal to 5, 10, 20. In these tests, we discretize each wavelength with  $q = 8$  points and the number of samples in each dimension is  $n = 39, 79, 159$ . The  $\alpha$  value of the modified system is set to be equal to 1. The width of the PML is equal to  $6h$  (i.e.,  $b = 6$ ) and the number of layers processed within each iteration of Algorithms 4.1 and 4.2 is equal to 3 (i.e.,  $d = 3$ ). The preconditioner sweeps the domain with two fronts that start from  $x_3 = 0$  and  $x_3 = 1$ .

The results of the first velocity field is reported in Table 8. The two plots show the solutions of the two right sides on a plane near  $x_1 = 0.5$ .  $T_{\text{setup}}$  is the time used to construct the preconditioner in seconds.  $N_{\text{iter}}$  is the number of iterations of the preconditioned GMRES iteration and  $T_{\text{solve}}$  is the solution time. The estimate in Section 4 section shows that the setup time scales like  $O(N^{4/3})$ . So when  $\omega$  doubles,  $N$  increases by a factor of 4 and  $T_{\text{setup}}$  should increase by a factor of 16. The numerical results show that the actual growth factor is even lower. A remarkable feature of the sweeping preconditioner is that in all cases the

preconditioned GMRES solver converges in at most 12 iterations. Finally, we would like to point out that our algorithm is quite efficient: for the case with  $\omega/(2\pi) = 20$  with more than four million unknowns, the solution time is less than 600 seconds. The results of the second and the third velocity fields are reported in Tables 9 and 10, respectively. In all tests, the GMRES iteration converges at most 13 iterations when combined with the new sweeping preconditioner.

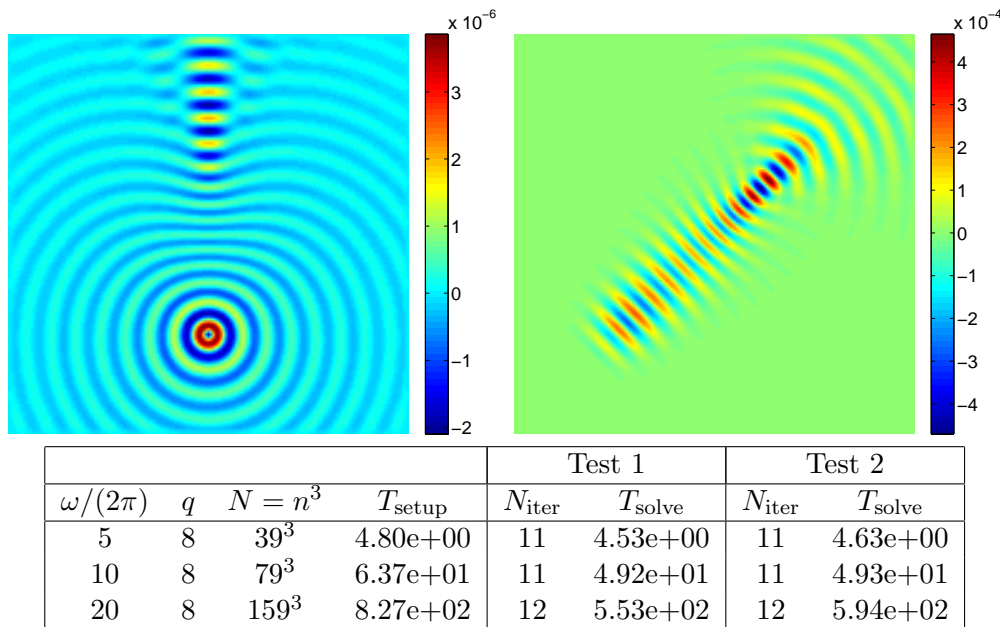


Table 8: Results of velocity field 1 with varying  $\omega$ . Top: Solutions for two external forces with  $\omega/(2\pi) = 16$  on a plane near  $x_1 = 0.5$ . Bottom: Results for different  $\omega$ .

Secondly, we study how the sweeping preconditioner behaves when  $q$  (the number of discretization points per wavelength) varies. We fix  $\frac{\omega}{2\pi}$  to be 5 and let  $q$  be 8, 16, 32. The test results for the three velocity fields are summarized in Tables 11, 12, and 13, respectively. These results show that the number of iterations remains roughly constant and the running time of the solution algorithm scales roughly linearly with respect to the number of unknowns.

Let us compare these numerical results with the ones from the 3D results from the previous paper [12]. The setup time  $T_{\text{setup}}$  of the current algorithms is much lower: for the problem of 20 wavelength across, the current setup time is in the hundreds of seconds while the setup time in [12] is in the tens of thousands of seconds. This is mainly due to the fact that our implementation of the multifrontal algorithm in this paper is more efficient compared to our implementation of the 2D hierarchical matrix algebra in [12]. The number of iterations  $N_{\text{iter}}$  is about 5 times larger, again due to the fact that the current algorithms use physical arguments about the Helmholtz equation rather than direct numerical approximation for  $T_m$ . Notice that the solution time  $T_{\text{solve}}$  is only about 3 to 4 times larger and this is due to the efficiency of applying  $\tilde{T}_m$  using the multifrontal factorization.

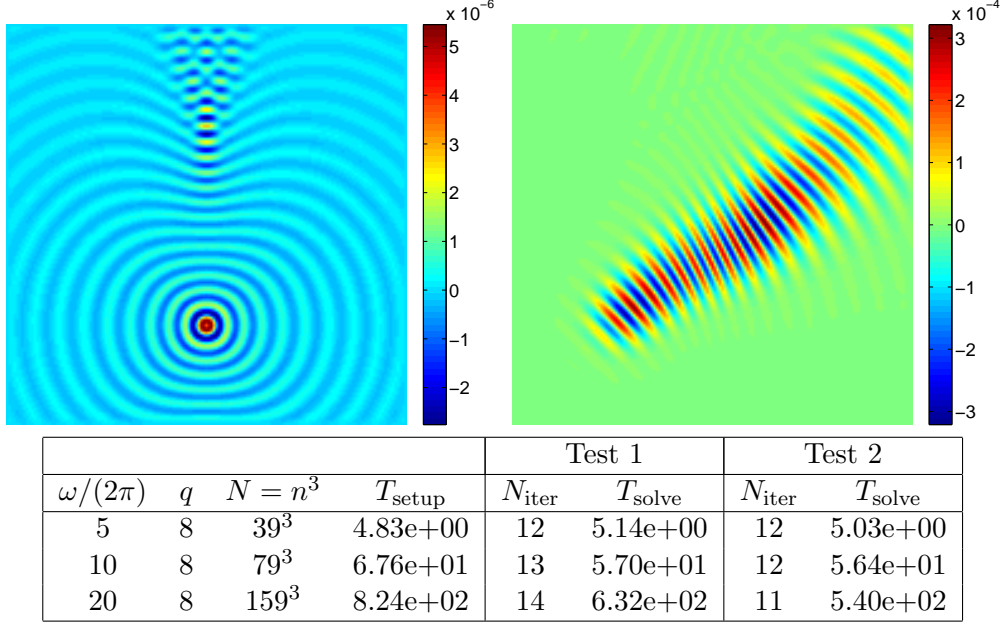


Table 9: Results of velocity field 2 with varying  $\omega$ . Top: Solutions for two external forces with  $\omega/(2\pi) = 16$  on a plane near  $x_1 = 0.5$ . Bottom: Results for different  $\omega$ .

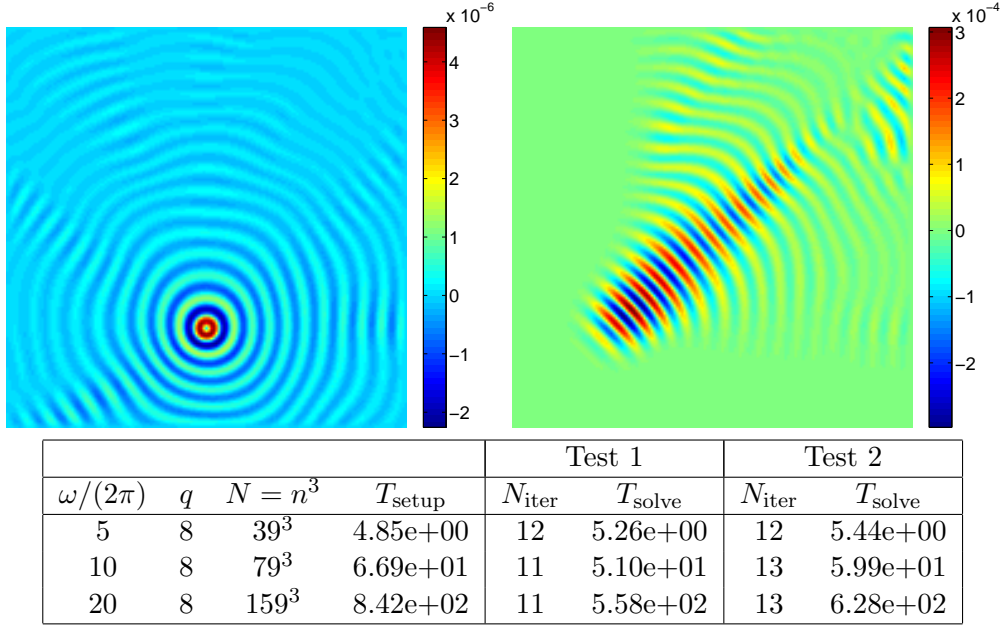


Table 10: Results of velocity field 3 with varying  $\omega$ . Top: Solutions for two external forces with  $\omega/(2\pi) = 16$  on a plane near  $x_1 = 0.5$ . Bottom: Results for different  $\omega$ .

## 6 Conclusion and Future Work

In this paper, we proposed a new sweeping preconditioner for the Helmholtz equation in two and three dimensions. Similar to the previous paper [12], the preconditioner is based on an

				Test 1		Test 2	
$\omega/(2\pi)$	$q$	$N = n^3$	$T_{\text{setup}}$	$N_{\text{iter}}$	$T_{\text{solve}}$	$N_{\text{iter}}$	$T_{\text{solve}}$
5	8	$39^3$	4.87e+00	11	4.91e+00	11	4.96e+00
5	16	$79^3$	6.59e+01	11	4.70e+01	12	5.55e+01
5	32	$159^3$	8.07e+02	13	5.91e+02	13	6.31e+02

Table 11: Results of velocity field 1 with varying  $q$ .

				Test 1		Test 2	
$\omega/(2\pi)$	$q$	$N = n^3$	$T_{\text{setup}}$	$N_{\text{iter}}$	$T_{\text{solve}}$	$N_{\text{iter}}$	$T_{\text{solve}}$
5	8	$39^3$	4.80e+00	12	5.36e+00	12	4.95e+00
5	16	$79^3$	6.74e+01	13	5.53e+01	12	5.51e+01
5	32	$159^3$	8.18e+02	14	6.48e+02	14	6.45e+02

Table 12: Results of velocity field 2 with varying  $q$ .

				Test 1		Test 2	
$\omega/(2\pi)$	$q$	$N = n^3$	$T_{\text{setup}}$	$N_{\text{iter}}$	$T_{\text{solve}}$	$N_{\text{iter}}$	$T_{\text{solve}}$
5	8	$39^3$	4.82e+00	12	4.92e+00	12	5.08e+00
5	16	$79^3$	6.77e+01	12	5.17e+01	13	6.04e+01
5	32	$159^3$	8.16e+02	13	6.26e+02	15	7.14e+02

Table 13: Results of velocity field 3 with varying  $p$ .

approximate block  $LDL^t$  factorization that eliminates the unknowns layer by layer starting from an absorbing layer or boundary condition. What is new is that the Schur complement matrices of the block  $LDL^t$  factorization are approximated by introducing moving PMLs in the interior of the domain. In the 2D case, applying these Schur complement matrices corresponds to solving quasi-1D problems by an LU factorization with optimal ordering. In the 3D case, applying these Schur complement matrices corresponds to solving quasi-2D problems with multifrontal methods. The resulting preconditioner has a linear application cost and the number of iterations is essentially independent of the number of unknowns or the frequency when combined with the GMRES solver.

Some questions remain open. First, we tested the algorithms with the PML boundary condition as the numerical implementation of the Sommerfeld condition. Many other boundary conditions are available and we believe that the current algorithms should work for these boundary conditions. We presented the algorithms using the simplest central difference scheme (5 point stencil in 2D and 7 point stencil in 3D). The dispersion relationships of these schemes are rather poor approximations to the true one. One would like to investigate other more accurate stencils and other types of discretizations such as finite element, spectral element, and discontinuous Galerkin.

Parallel processing is necessary for large scale 3D problems. Although the overall structure of the sweeping preconditioner is sequential by itself, the calculation of the multifrontal method within each iteration can be well parallelized. Several efficient implementations are already available [1, 20] for this purpose. There is also an alternative to parallelize via a coarse scale domain decomposition and apply our technique within each subdomain.

The approach of the current paper is readily applicable to non-uniform and even adaptive grids. In fact, the same non-uniform or adaptive grid can be used for the subproblems associated with the moving PMLs, as long as the grid can resolve the moving PML with sufficient accuracy. Since the multifrontal methods for non-uniform and adaptive grids are readily available [1, 21], it makes the current approach more flexible compared with the one of the previous paper [12] based on the hierarchical matrix representation.

## References

- [1] P. R. Amestoy, I. S. Duff, J.-Y. L'Excellent, and J. Koster. A fully asynchronous multifrontal solver using distributed dynamic scheduling. *SIAM J. Matrix Anal. Appl.*, 23(1):15–41 (electronic), 2001.
- [2] A. Atle and B. Engquist. On surface radiation conditions for high-frequency wave scattering. *J. Comput. Appl. Math.*, 204(2):306–316, 2007.
- [3] A. Bayliss, C. I. Goldstein, and E. Turkel. An iterative method for the Helmholtz equation. *Journal of Computational Physics*, 49(3):443 – 457, 1983.
- [4] J.-D. Benamou and B. Després. A domain decomposition method for the Helmholtz equation and related optimal control problems. *J. Comput. Phys.*, 136(1):68–82, 1997.
- [5] J.-P. Berenger. A perfectly matched layer for the absorption of electromagnetic waves. *J. Comput. Phys.*, 114(2):185–200, 1994.
- [6] A. Brandt and I. Livshits. Wave-ray multigrid method for standing wave equations. *Electron. Trans. Numer. Anal.*, 6(Dec.):162–181 (electronic), 1997. Special issue on multilevel methods (Copper Mountain, CO, 1997).
- [7] W. C. Chew and W. H. Weedon. A 3-d perfectly matched medium from modified Maxwell's equations with stretched coordinates. *Microwave Opt. Tech. Lett.*, 7:599–604, 1994.
- [8] B. Després. Domain decomposition method and the Helmholtz problem. In *Mathematical and numerical aspects of wave propagation phenomena (Strasbourg, 1991)*, pages 44–52. SIAM, Philadelphia, PA, 1991.
- [9] J. Duff and J. Reid. The multifrontal solution of indefinite sparse symmetric linear equations. *ACM Trans. Math. Software*, 9:302–325, 1983.
- [10] H. C. Elman, O. G. Ernst, and D. P. O'Leary. A multigrid method enhanced by Krylov subspace iteration for discrete Helmholtz equations. *SIAM J. Sci. Comput.*, 23(4):1291–1315 (electronic), 2001.
- [11] B. Engquist and L. Ying. Fast directional multilevel algorithms for oscillatory kernels. *SIAM J. Sci. Comput.*, 29(4):1710–1737 (electronic), 2007.
- [12] B. Engquist and L. Ying. Sweeping preconditioner for the Helmholtz equation: hierarchical matrix representation. preprint, 2010.
- [13] Y. A. Erlangga. Advances in iterative methods and preconditioners for the Helmholtz equation. *Arch. Comput. Methods Eng.*, 15(1):37–66, 2008.



- [14] Y. A. Erlangga, C. W. Oosterlee, and C. Vuik. A novel multigrid based preconditioner for heterogeneous Helmholtz problems. *SIAM J. Sci. Comput.*, 27(4):1471–1492 (electronic), 2006.
- [15] J. George. Nested dissection of a regular finite element mesh. *SIAM J. Numer. Anal.*, 10:345–363, 1973.
- [16] W. Hackbusch. A sparse matrix arithmetic based on  $\mathcal{H}$ -matrices. Part I: Introduction to  $\mathcal{H}$ -matrices. *Computing*, 62:89–108, 1999.
- [17] S. Johnson. Notes on perfectly matched layers. Technical Report, Massachusetts Institute of Technology, 2010.
- [18] G. A. Kriegsmann, A. Taflove, and K. R. Umashankar. A new formulation of electromagnetic wave scattering using an on-surface radiation boundary condition approach. *IEEE Trans. Antennas and Propagation*, 35(2):153–161, 1987.
- [19] A. Laird and M. Giles. Preconditioned iterative solution of the 2D Helmholtz equation. Technical Report, NA 02-12, Computing Lab, Oxford University, 2002.
- [20] L. Lin, C. Yang, J. Lu, L. Ying, and W. E. A fast parallel algorithm for selected inversion of structured sparse matrices with application to 2D electronic structure calculations. Submitted, 2010.
- [21] L. Lin, C. Yang, J. Meza, J. Lu, L. Ying, and W. E. Selinv—an algorithm for selected inversion of a sparse symmetric matrix. Submitted, 2010.
- [22] J. Liu. The multifrontal method for sparse matrix solution: Theory and practice. *SIAM Rev.*, 34:82–109, 1992.
- [23] D. Osei-Kuffuor and Y. Saad. Preconditioning Helmholtz linear systems. Technical Report, umsi-2009-30, Minnesota Supercomputer Institute, University of Minnesota, 2009.
- [24] V. Rokhlin. Diagonal forms of translation operators for the Helmholtz equation in three dimensions. *Appl. Comput. Harmon. Anal.*, 1(1):82–93, 1993.
- [25] Y. Saad. *Iterative methods for sparse linear systems*. Society for Industrial and Applied Mathematics, Philadelphia, PA, second edition, 2003.
- [26] Y. Saad and M. H. Schultz. GMRES: a generalized minimal residual algorithm for solving nonsymmetric linear systems. *SIAM J. Sci. Statist. Comput.*, 7(3):856–869, 1986.